Review

Institution of MECHANICAL ENGINEERS

Journal of RAIL AND RAPID TRANSIT

An analysis of resonance effects in locomotive drive systems experiencing wheel/rail saturation adhesion

Proc IMechE Part F:
J Rail and Rapid Transit
2014, Vol 228(1) 4–15

DOI: 10.1177/0954409712457519
pif.sagepub.com
SAGE

Yuan Yao, Hong-jun Zhang and Shi-hui Luo

Abstract

This study investigates the dynamic response of a locomotive drive system experiencing wheel/rail saturation adhesion. A dynamic locomotive model is created and then integrated with electromechanical and control systems to simulate the vibration in the component parts of the drive system. The model is used to investigate the drive system's sensitivity to resonance effects. The obtained results show that the wheel/rail stick-slip state can experience both longitudinal vibrations and self-excited vibrations in the drive system. Different parts of the drive system are excited by the two types of vibrations; however, in both cases the main frequencies are multiples of the natural frequency vibration of the drive system. It is necessary to select an appropriate value for the motor suspension rubber stiffness if structural resonances of the drive system under wheel/rail saturated adhesion are to be avoided.

Keywords

Locomotive, dynamics of a drive system, stick-slip vibration, self-excited vibration, saturated adhesion

Date received: 22 December 2011; accepted: 17 July 2012

Introduction

The traction weight of heavy-duty trains in China has reached 20,000 tons; this requires the use of high-powered railway locomotives which in turn requires a detailed understanding of the effects of wheel/rail adhesion. The saturation and negative slope characteristics evident in adhesion curves can cause complex dynamic problems in high-powered locomotives. The drive system is a key component that represents the technical level of the locomotive bogie. The existing literature on the theoretical analysis of locomotive drive systems has focused on drive system dynamics including stick-slip vibration and stability[1–4] and the self-excited vibration[5–8] experienced by drive systems caused by the negative slope in wheel/rail adhesion curves.[9–12] There is only a sparse literature that addresses the structure vibration characteristics of the drive equipment as a function of drive condition. Lata[13] has summarized the types of drive systems used in modern locomotives and investigated the torsional dynamics of these drive systems. An in-depth study of the structure vibrations which occur in drive systems under the condition of wheel/rail saturation adhesion is of particular interest. In this paper, first, typical wheel/rail dynamic characteristics are investigated, and then a dynamic locomotive model is integrated with electromechanical and control systems to simulate the vibration of the component parts in the drive system. Their main frequencies are then calculated. The interaction vibration rules of different parts are analyzed and parameter matching principles to avoid resonance of the drive systems are summarized.

The dynamic characteristics under saturation adhesion

The self-excited vibration of the drive system

As a result of the lateral motion of wheelsets caused by track irregularities, both sides of a wheel experience alternating longitudinal tangential forces in addition to traction and this leads to changes in the wheel/rail stick-slip states as shown in Figure 1. The shown data was obtained in simulations using the SIMPACK program with a modified creep force obtained using equation (1), see the section "The effect of wheel/rail adhesion characteristics on saturation adhesion," for an axle load of the locomotive of 25 t running on an ideal track i.e. it has a Kalker

Traction Power State Key Laboratory, Southwest JiaoTong University, People's Republic of China

Corresponding author:
Yuan Yao, Traction Power State Key Laboratory, Southwest JiaoTong University, Chengdu 610031, People's Republic of China.
Email: yyuan8848@163.com

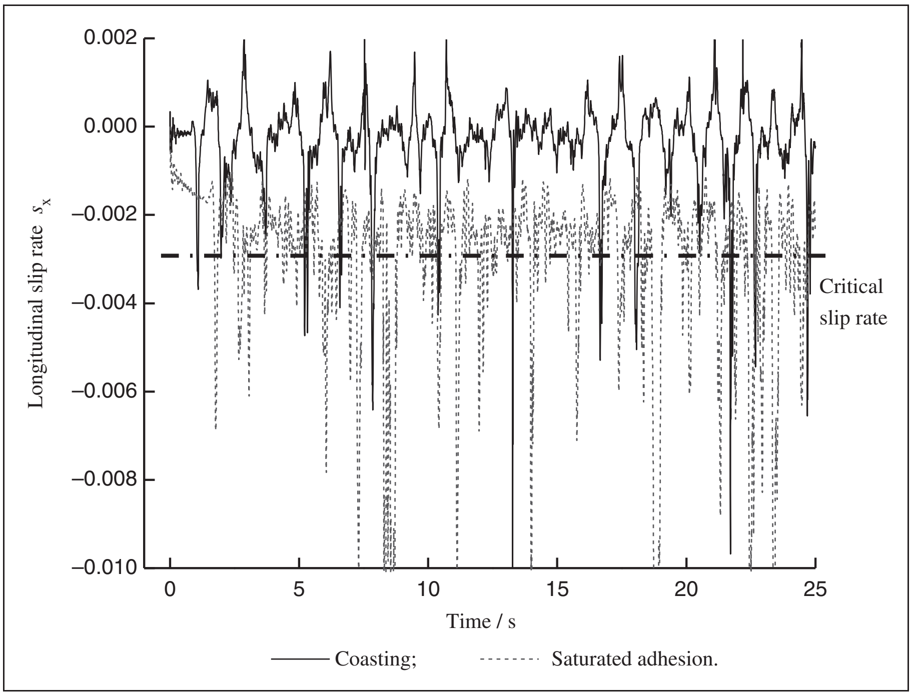

Figure 1. The longitudinal slip rates of the coasting and saturated adhesion states.

weight coefficient of one. When the relative displacement between the wheel and the rail is small, such as during coasting, the adhesion state of the wheelset is stable. With an increase in drive torque or deterioration of the track surface conditions, the adhesion state of the wheelset becomes unstable as a result of the negative slope observed in adhesion curves when a macroscopic slip between the wheel and rail occurs. This is different from wheel/rail creepage in classic vehicle system dynamics. Since a locomotive's wheelsets can easily slip, the degree of wheel slide can be defined as the slip rate.[1] The expression for the slip rate is the same as that for the creepage, the denominator being the longitudinal speed of the wheel but in this case it is the average speed, which is highly suitable for the definition of wheel spin. The slip rate is a variable of the dynamic locomotive system. Under a saturation adhesion state of the wheel, the critical slip rate that corresponds to the wheel/rail adhesion peak can be easily exceeded. The unstable slide of the wheel leads to self-excited vibration in the locomotive drive system with the main frequency of these vibrations being the natural frequency. Figure 2 shows the acceleration spectrum of the wheelset's torsional vibration under wheel spin for the locomotive.[8] The main vibration frequency is the natural torsional vibration frequency of the wheelset.

In the dynamic system, the slip rate (S) is equal to the sum of the mean slip rate (S_0) and the dynamic slip rate ds. The value of s_0 depends on the traction working condition and the wheel/rail adhesion state. Figure 3 shows the changes in adhesion stability under wheel/rail stick-slip. The symbol a represents the stick state, b represents the stick-slip state and c represents the slip state. Ignoring structure damping, the vibrations in the stick state are stable because the positive damping of wheel/rail adhesion dissipates energy and vice versa. For conditions b and c, as the system energy increases, the amplitude of ds will increase until s is located in a positive slope region of the adhesion curve. In other words, when the system is in a stick-slip vibration state, the processes of increasing and consumption of system energy are in balance, and vibration exists within the limit cycle. Under condition c, the value of s_0 is greater than that in condition b, and a larger input energy makes it easier to change the wheelset from slippage to stick-slip.

For a locomotive in service, s_0 cannot be a constant, and ds cannot increase infinitely. In Figure 3, comparing a' with a, since the structure stiffness and damping of the drive system are smaller and the vibration scope of s is wider comparatively, the stick state changes into a stick-slip state and as a result vibrations develop more easily. This increases the system's vibrational energy and it reaches the slip state more quickly. Likewise, when the running state of the wheelset changes from slip to stick, the wide vibration scope of s increases the time required for re-adhesion.

Many factors influence the re-adhesion of the locomotive, such as rail surface condition, locomotive structural parameters, electric drive system and the mechanical characteristics of the engine. Among these factors, decreasing the mean slip and the dynamic slip rates are key approaches to increase the locomotive's re-adhesion ability.

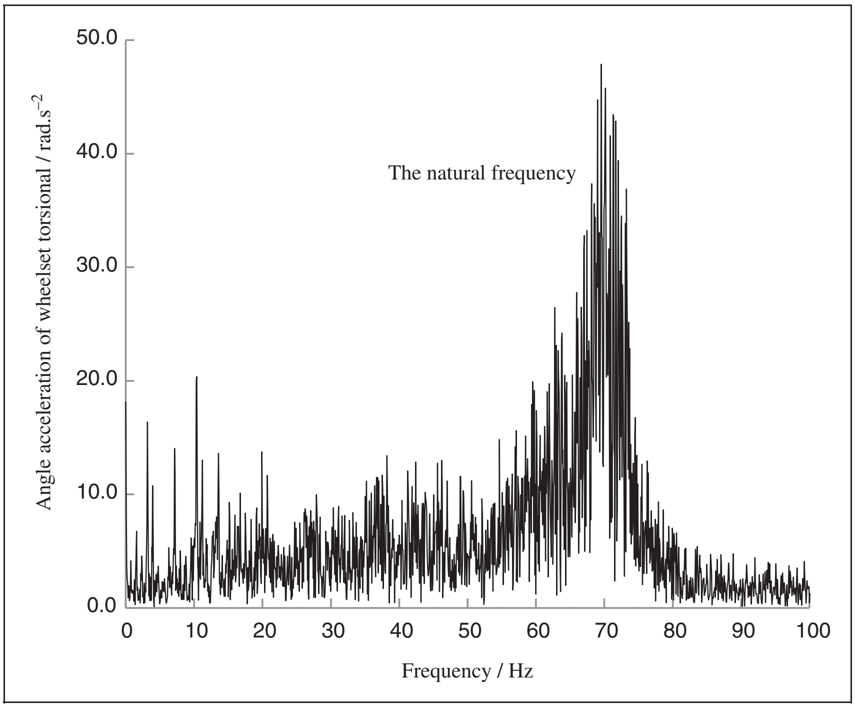

Figure 2. The acceleration spectrum of the torsional vibration of the wheelset when the wheels spin.

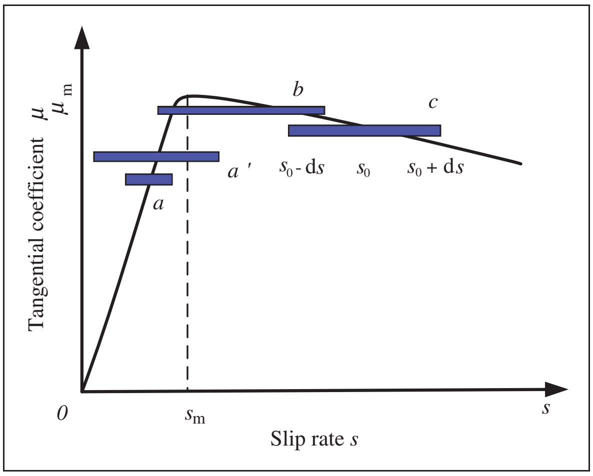

Figure 3. The stick-slip vibration analysis.

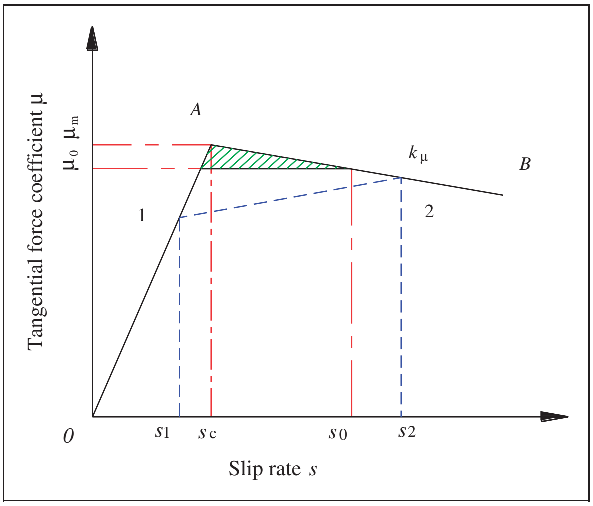

Figure 4. Analysis of the longitudinal vibration mechanism of the wheelset.

The longitudinal vibration in the wheelset

Ignoring the damping effect from the locomotive's drive system and inertia, if the slip rate is located in the OA section in Figure 4 and the motor torque is a constant, then positive damping will decrease the system's energy content, and the angular acceleration of the wheelset will be negative. However, if the slip rate is located in the AB section, the angular acceleration will be positive. When the tangential force coefficient is greater than the value of mean tangential force coefficient (u_0) during the periodic vibration process, which corresponds to the shaded area in Figure 4, the acceleration of the longitudinal vibration of the wheelset is positive, and vice versa. During the stick-slip process of the wheelset, the minimum and maximum slip rates are located on either side of s_0, respectively. The minimum value is less than s_c, as shown in Figure 4. Points 1 and 2 are the corresponding tangential force coefficients of s_1 and s_2, respectively. If the slip rate changes during a cycle of s_1–s_2–s_1, then the angular velocity of the wheelset will display the following characteristics: decrease–increase–decrease. However, the change process of the velocity of the longitudinal

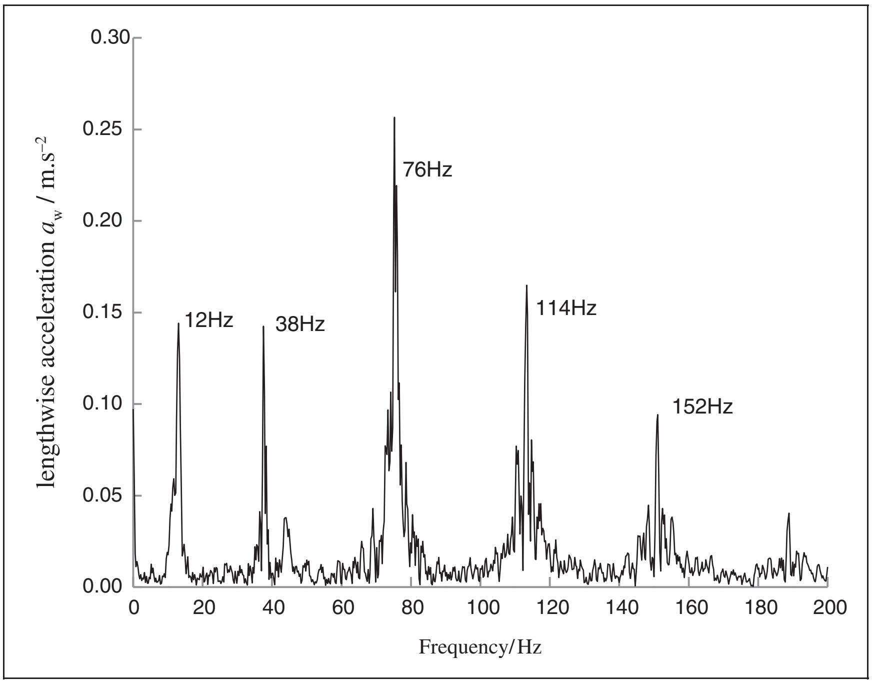

Figure 5. Acceleration/frequency spectrum of the longitudinal vibration of the wheelset.

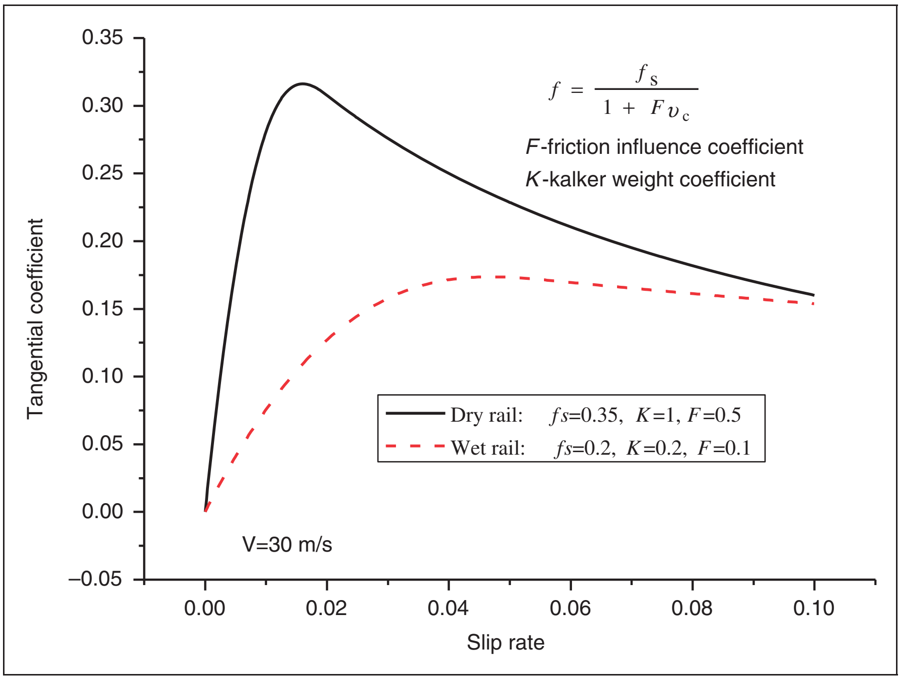

Figure 6. The tangential force curves for different *K* and *F* values.

vibration of the wheelset is decrease–increase–decrease–increase–decrease. The wave frequency of the acceleration of the longitudinal vibration of the wheelset is double the frequency of the acceleration of the vibration due to the rotation of the wheelset.

Figure 5 shows the acceleration/frequency spectrum of the longitudinal vibration of the wheelset, where 12 Hz is the natural frequency of the longitudinal vibration and 38 Hz is the main frequency of the torsional vibration and the natural frequency of the drive system. The longitudinal vibration frequencies of the wheelset contain the natural frequency and its integral is in multiples of the torsional vibration of the drive system. The vibration energy reaches a maximum of twice the natural frequency.

If matching the torsional stiffness of the drive system and the longitudinal axle guidance stiffness of the locomotive is unreasonable, and if the frequency

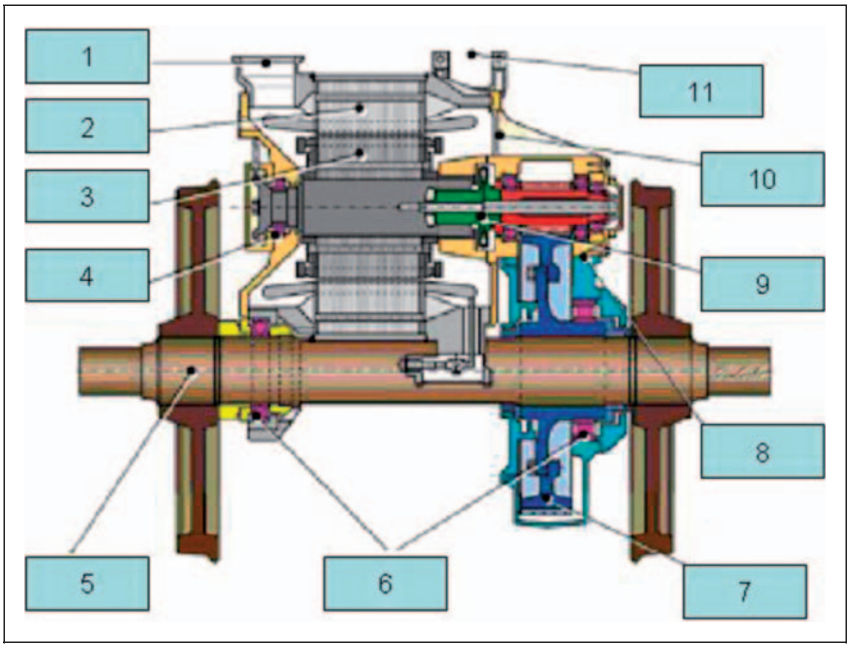

Figure 7. The axle-mounted drive system. 1 - air inlet; 2 - stator; 3 - rotor; 4 - motor bearing; 5 - shaft; 6 - bearing; 7 - large gear; 8 - interface; 9 - coupling; 10 - air outlet; 11 - suspension.

of the longitudinal vibration of the wheelset is an integral multiple of the rotation vibration frequency, then stick-slip vibration will cause a strong longitudinal resonance in the wheelset. This strong resonance indicates large dynamic loads, and wheel tread spalling or potential safety problems may occur.

The effect of wheel/rail adhesion characteristics on saturation adhesion

The tangential force coefficient decreases in response to an increase in the wheel/rail slip velocity. This corresponds to a negative slope characteristic in the adhesion curve. According to some investigations, adhesion curves are different under different rail surface conditions. These differences include:

- a maximum tangential force coefficient;
- a slip rate that corresponds to this maximum tangential force coefficient;
- a linear slope near the origin;
- a negative slope at slippage.

These can be defined as the four factors of adhesion. The wheel/rail friction coefficient f is a function of the contact patch sliding velocity and can be written as[14]

$$f = \frac{f_s}{1 + F\upsilon_c} \tag{1}$$

where f_s is the static friction coefficient, F is the dynamic friction coefficient which corresponds to the effect of the contact sliding velocity on the friction coefficient and υ_c is the sliding velocity of the contact patch.

Modifying the wheel/rail tangential force calculation program of Shen et al.[15] by incorporating equation (1) allows wheel/rail tangential force coefficient curves to be obtained that include the negative slope characteristic. Changing the Kalker weight coefficient K and the friction influence coefficient F enables the four factors of the adhesion curves to be simulated. The obtained tangential force coefficient curves are shown in Figure 6.

The model of the dynamics of a high-power locomotive

The model of the dynamics of the train system was created using the software SIMPACK. The model considered a locomotive with 10 vehicles, the hauled load was considered and each vehicle was simulated as a mass block. This mass block had a single degree of freedom along the track direction, and the mass blocks were connected by a coupler force. The axle load of the locomotive and the vehicle were 23 t and 21 t, respectively. The locomotive was equipped with a Co′Co′ axle arrangement and the uniaxial power was 1600 kW. The locomotive drive system was taken to have an integral structure, which means that the gear box is installed on the wheelset and can rotate around it. The motor was suspended under the frame by a rod such as the one shown in Figure 7. The drive system model included a motor, a gearbox, a rotor, a hang rod, a pinion and a large gear; their degrees of freedom are listed in Table 1. The high-power locomotive drive system used flexible coupling between rotor and pinion.

Table 1. The degrees of freedom of the elements used in the model of the dynamics of the locomotive.

Element	Lengthwise	Lateral	Vertical	Roll	Pitch	Yaw
Car	X_c	Y_c	Z_c	Φ_c	θ_c	Ψ_c
Frame	X_{fi}	Y_{fi}	Z_{fi}	Φ_{fi}	θ_{fi}	Ψ_{fi}
Motor (gearbox)					θ_{bj}*	
Hang rod				Φ_{rj}	θ_{rj}	
Rotor					θ_{mj}	
Small gear					θ_{gj}	
Wheelset (big gear)	X_{wj}	Y_{wj}	Z_{wj}*	Φ_{wj}*	θ_{wj}	Ψ_{wj}
Vehicle	X_{vk}					

Note: the symbol * denotes dependent freedoms: $i = 1–2$, $j = 1–6$, $k = 1–10$.

Table 2. The main vibration frequencies (in Hz) under different conditions.

	Curved track			Straight line		
Freedom	Coasting	Driving	Saturation adhesion	Coasting	Driving	Saturation adhesion
Wheelset longitudinal	12	12	12,62	12	12	12,62
Bogie frame longitudinal	24	24	24,62	24	24	24,62
Motor pitching	62	62	26,62	62	62	26,62
Wheelset torsion	–	82,62	82,62	–	82,62	82,62
Wheelset rotation	62	62	26,62	62	62	26,62
Motor rotor rotation	–	26	26	–	26	26

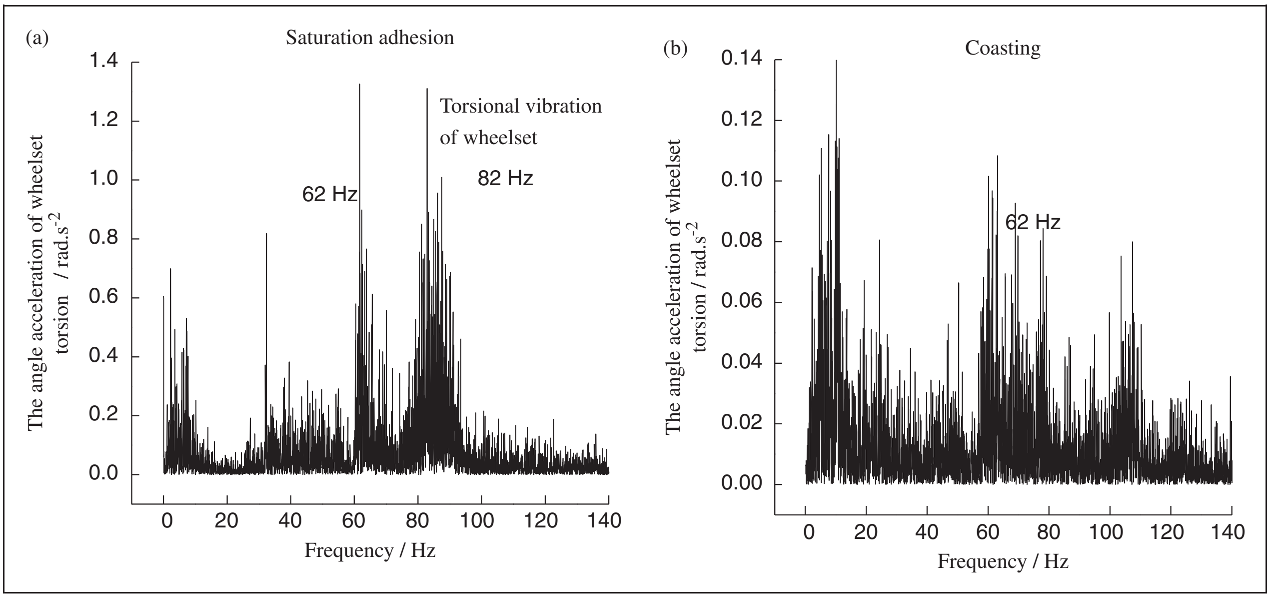

Figure 8. The torsional vibration of the wheelset (a) saturation adhesion and (b) coasting.

By taking the train running environment into account, the train resistance can be taken to be composed of the basic resistance and the additional resistance of the ramp way. The train runs uniformly when the locomotive traction force and resistance are balanced. The unit weight resistance can be written as

$$w = a + b \times v + c \times v^2 + i \tag{2}$$

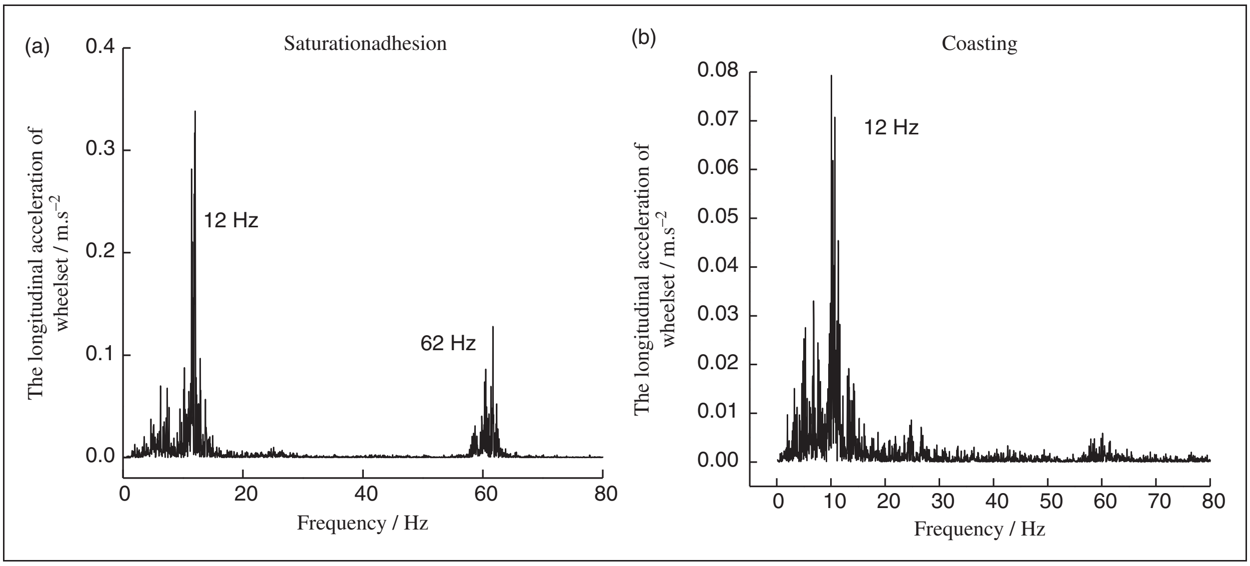

Figure 9. The longitudinal vibration of the wheelset (a) saturation adhesion and (b) coasting.

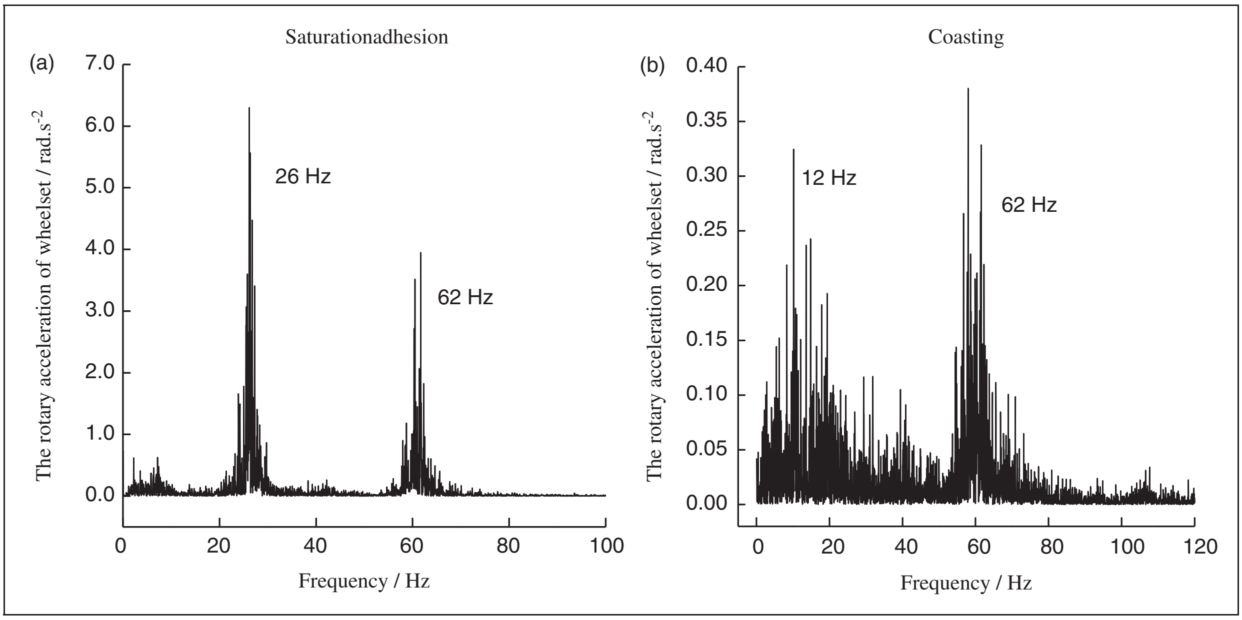

Figure 10. The rotary vibration of the wheelset (a) saturation adhesion and (b) coasting.

where a,b,c are resistance coefficients, v is the train speed and i is the slope of the gradient way. In this section, a USA 5 class track irregularity, JM3 worn-type wheel profile and standard 60 kg/m rail shape are adopted.

The dynamics model can simulate actual dynamic processes during the locomotive traction operation. This model can cover more uncertain factors in the locomotive adhesion control than a simple mechanical model with a single wheel.

The vibration frequency analysis of the locomotive drive

With the proposed model and appropriate control strategies,[16–18] the virtual locomotive runs under saturation adhesion. For the locomotive drive system, the considered vibration frequencies are between 10 and 90 Hz, thus low-frequency phenomena such as hunting and car-body suspension frequencies are not taken into account. The structural vibration includes the wheelset rotation, wheelset torsion, wheelset longitudinal vibration, motor and gearbox pitching, the rotor rotation and bogie frame longitudinal vibration. The main vibration frequencies of the drive systems under different running conditions are listed in Table 2. The track surface condition was taken to be a dry rail.

Figures 8 to 13 show the vibration acceleration/frequency spectra of the drive system under saturation adhesion and coasting conditions.

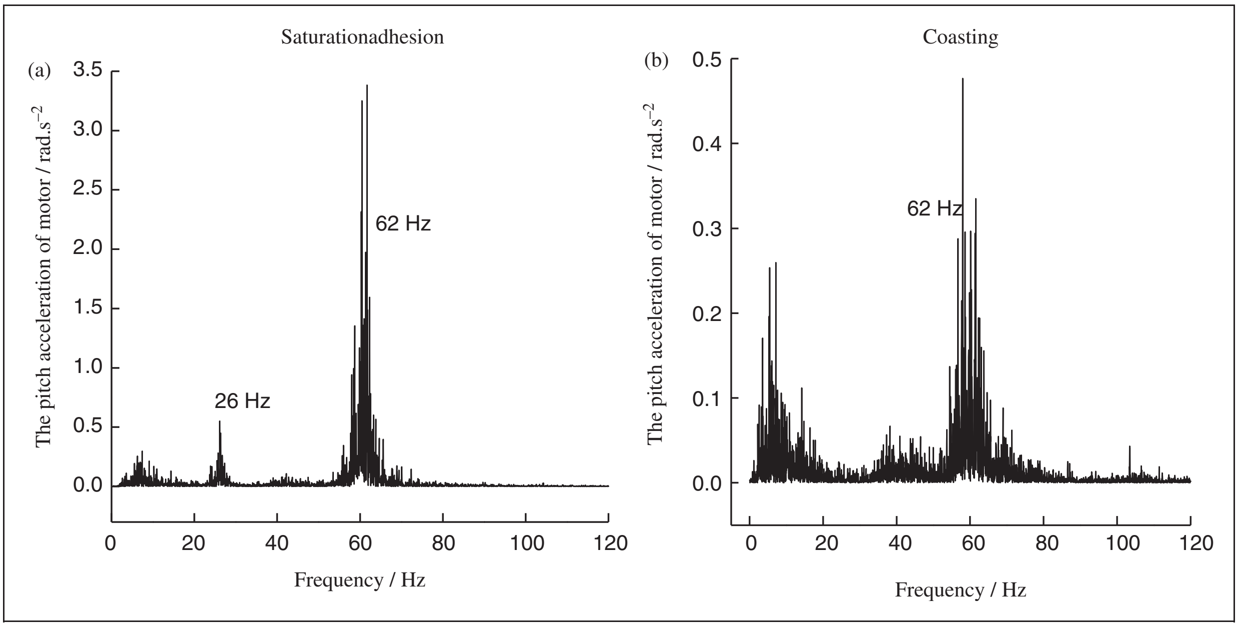

Figure 11. The pitch vibration of the motor (a) saturation adhesion and (b) coasting.

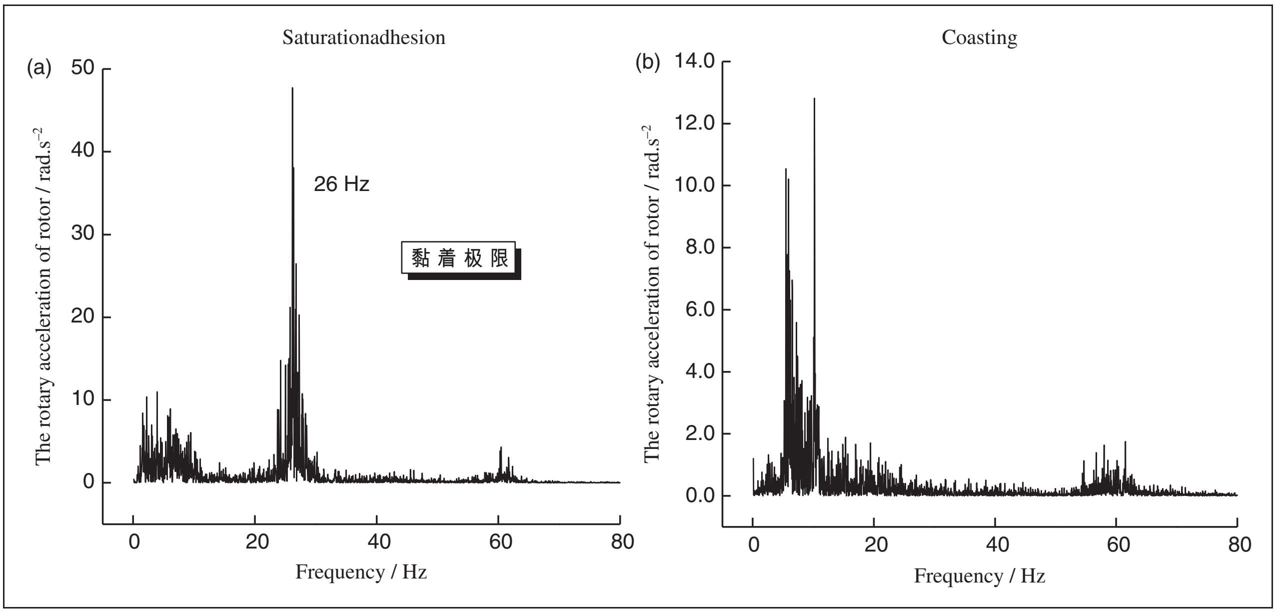

Figure 12. The rotary vibration of the rotor (a) saturation adhesion and (b) coasting.

The following points can be made after close scrutiny of the figures.

1. Under saturation adhesion, the main frequencies of the longitudinal, rotational and torsional vibrations of the wheelsets include the natural vibration frequency of the motor and gearbox pitching vibration (62 Hz).
2. The motor rotor and wheel rotation vibrations contain the main frequency (26 Hz) that is caused by the torsional stiffness of the flexible coupling.
3. Relative to the coasting condition, the vibration amplitude of the drive system is greater when the locomotive is under saturation adhesion.

Resonance analysis of the drive system

The relationships between the main vibration frequencies of the drive system

The simulations show that the main vibration frequencies of every part of the drive system contain the natural motor vibration frequency and the

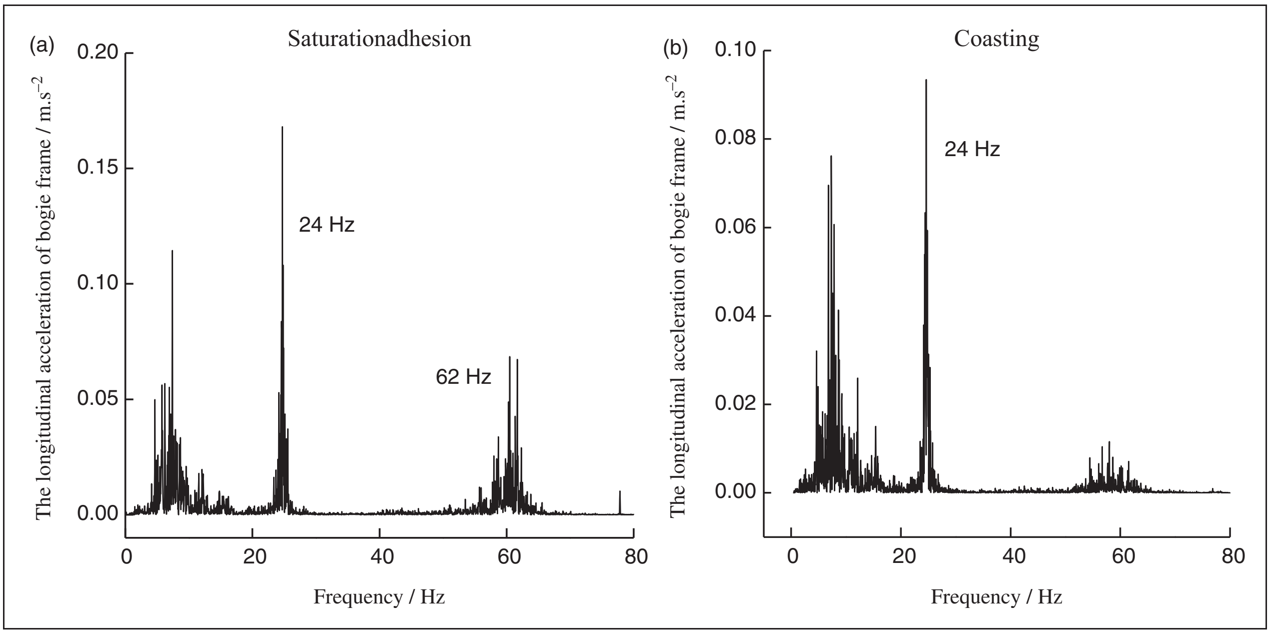

Figure 13. The longitudinal vibration of the bogie frame (a) saturation adhesion and (b) coasting.

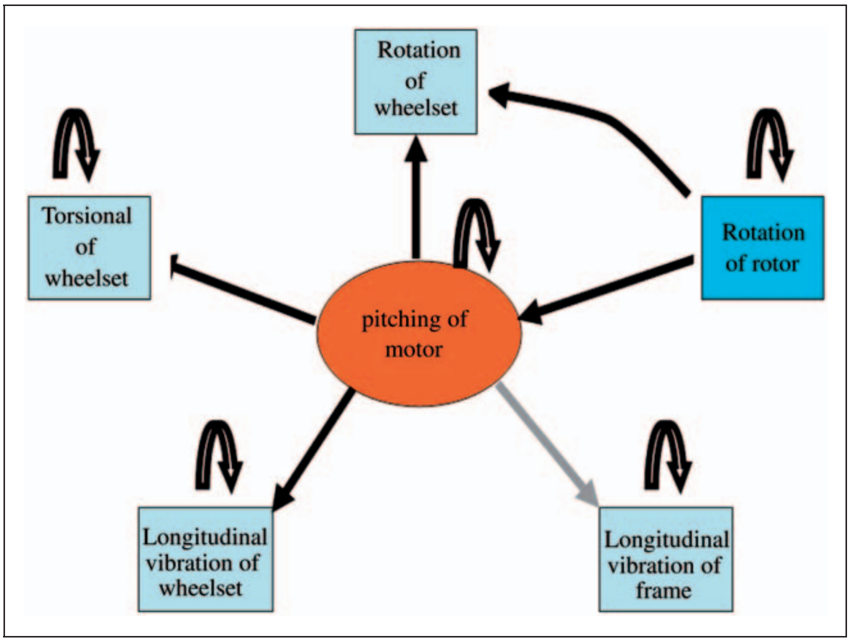

Figure 14. The relationships between the main vibration frequencies of the drive system.

gearbox pitching vibration. The main vibration frequencies occur when the locomotive is under saturation adhesion. If the natural vibration frequencies of other parts are equal to the pitching frequency of the motor and gearboxes, there will be a structural resonance. Figure 14 shows the relationship between the vibration frequencies of the main parts. A solid arrow indicates a vibration frequency that will appear in the main frequencies of the objective. A hollow arrow indicates the innate natural vibration frequencies of the parts. Once an object has two or more arrows pointing at it, it is a potential source of resonance. From this figure, the pitching vibration of the motor and gearboxes has a significantly impact.

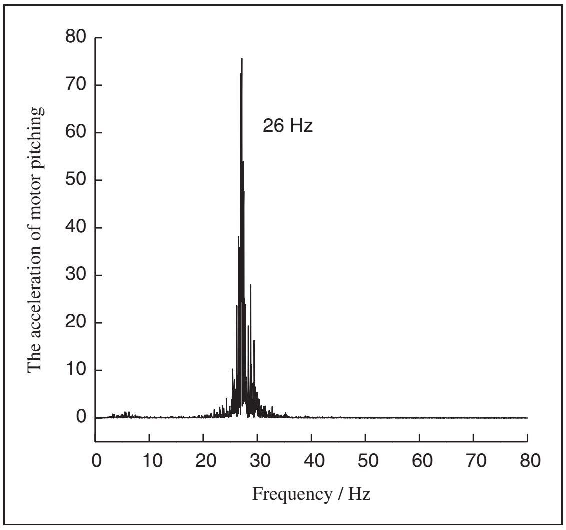

Figure 15. The pitching of the motor.

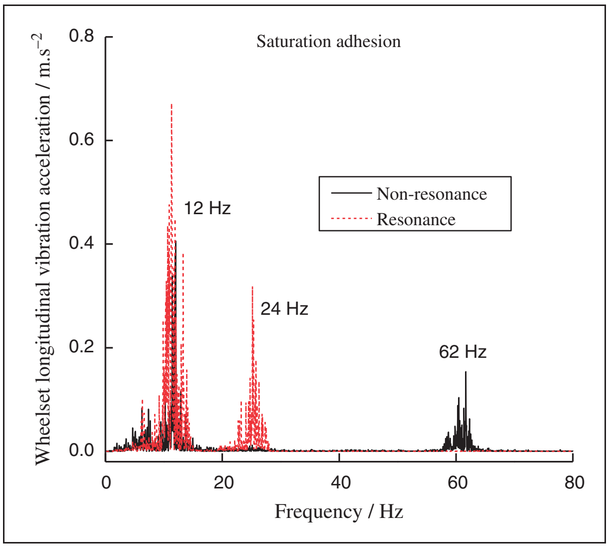

Figure 17. The wheelset's longitudinal vibrations showing that resonance occurs.

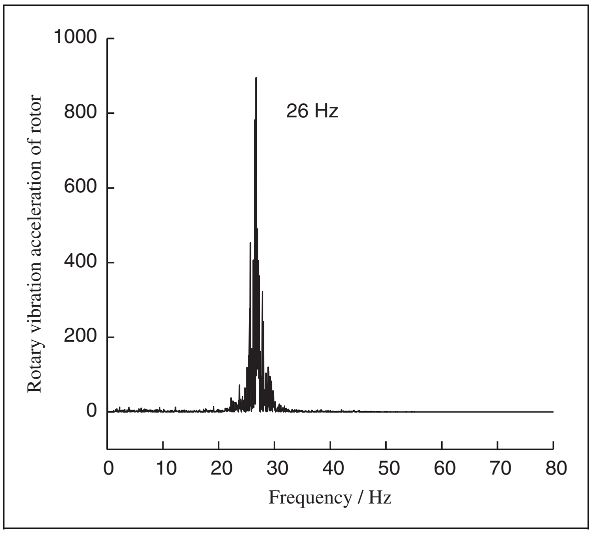

Figure 16. The vibrations of the rotor.

Thus, the optimization of the suspension stiffness of motors is not considered to affect the vibration of the other parts.

The resonance sensitivity of the drive system

From the preceding analysis, the pitching vibration frequency of the motor and gearbox is important. If the suspension stiffness of the motor is inappropriate then resonance will occur in the drive system. Resonance can lead to serious problems and thus the resonance sensitivity of the drive system when the locomotive is under saturation adhesion is investigated in this section.

The natural frequencies of the motor pitching and rotor rotation vibrations are the same. The suspension stiffness of the motor was changed to make the natural frequencies of the motor pitching and rotor rotation vibrations the same. The acceleration spectra for the motor pitching and rotor rotation vibrations are shown in Figures 15 and 16, respectively. The main vibration frequency of both is 26 Hz and their vibration amplitudes are very large. The resonance leads to serious damage of the drive system.

The natural frequencies of the motor pitching vibration and longitudinal vibration of the wheelset are the same. The suspension stiffness of the motor was changed to make the natural frequencies of the motor pitching and longitudinal vibration of the wheelset equal. The acceleration spectra of the motor pitching and the longitudinal vibrations of the wheelset are shown in Figure 17. The main vibration frequency of both occurs at 12 Hz and the amplitudes of the longitudinal vibration of the wheelset are large when resonance occurs. As in the previous analysis, the double frequency of the longitudinal vibration (24 Hz) is significant.

The natural frequencies of the motor pitching and torsional vibrations in the wheelset are the same. The suspension stiffness of the motor was changed to make the natural frequencies of the motor pitching and the torsional vibrations in the wheelset the same. The acceleration spectra of the torsional vibrations in the wheelset at resonance and in non-resonant conditions are shown in Figure 18. The main vibration frequency of both is 82 Hz, and the amplitude of the torsional vibration in the wheelset when resonance occurs is four times that in the non-resonance condition. The motor pitching and the torsional vibrations in the wheelset are sensitive to resonance.

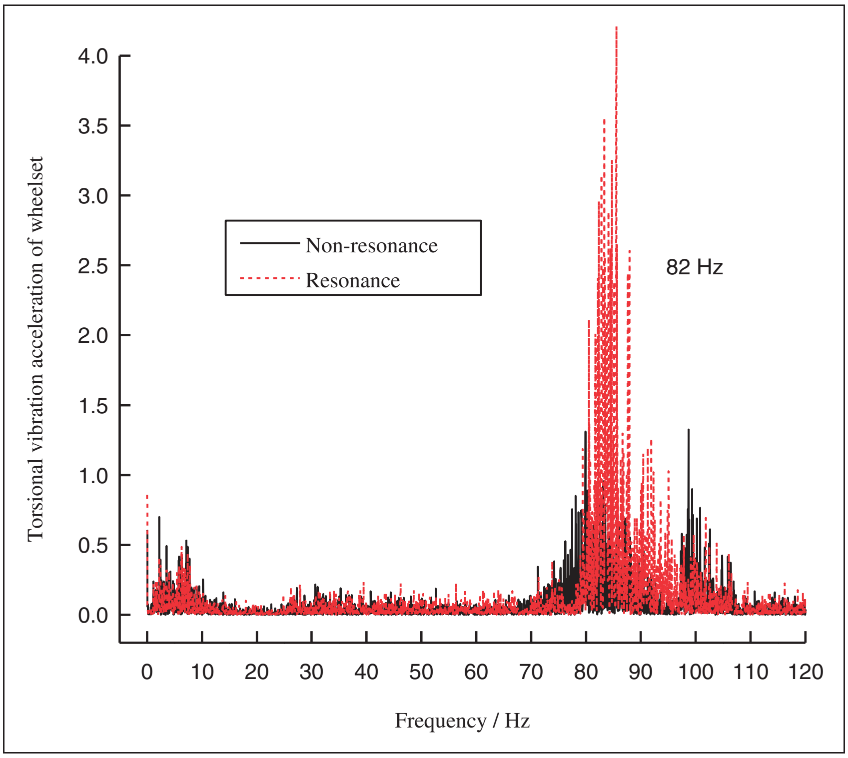

Figure 18. The wheelset's torsional vibrations showing that resonance occurs.

Conclusions

This paper studied the typical dynamic characteristics of a locomotive under saturation adhesion and analyzed the main vibration frequencies of the different parts of the drive systems and their relationship under coasting, driving and saturation adhesion states. The following conclusions can be drawn from the presented study.

1. Track irregularities and wheelset hunting make the left and right wheels run in a stick-slip state of locomotion under saturation adhesion. The stick-slip vibration results in the creation of longitudinal vibrations in the wheelset and self-excited vibrations in the drive system.
2. The self-excited vibration can cause intense vibrations in the drive system. The main vibration frequencies of the different parts of the drive system can affect each other resulting in resonance phenomena.
3. The pitching vibration of the motor and the gearbox significantly impact the drive system. Therefore, it is necessary to select an appropriate value for the motor suspension to avoid resonance conditions for the rotor rotation, wheelset torsional and longitudinal vibrations.
4. Particular attention must be given to ensure that the natural frequency of motor pitching is not the same as the vibration frequencies of the rotor rotation and the longitudinal vibration of the wheelset.

Funding

This research received funding from the National Natural Science Foundation of China (grant no. 51075339) and Independent Research and Development Projects of a Key Laboratory grant (grant no. 2011TPL_T04).

References

1. Yao Y, Zhang HJ and Li YM. The dynamic study of locomotives under saturated adhesion. *Veh Sys Dyn* 2011; 49: 1321–1338.
2. Wu YF. Stability analysis of the vibration of the frame-mounted motor driving system. *J China Railway Soc* 1992; 14: 1–7.
3. Muller S and Kogel R. Numerical simulation of roll-slip oscillations in locomotive drives. *Zeit Angew Math Mech* 2001; 8: 61–64.
4. Yao Y, Zhang HJ and Luo Y. Torsional-longitudinal coupling vibration analysis of drive system on locomotive. *J Traffic Transport Engng* 2009; 9: 13–17.
5. Hirotsu T, Kasai S and Takai H. Self-excited vibration during slippage of parallel cardan drives for electric railcars. *JSME Int J* 1987; 30: 304–1310.
6. Polach O. Influence of locomotive tractive effort on the forces between wheel and rail. *Veh Syst Dyn* 2001; 35: 7–22.
7. Yao Y, Zhang HJ and Luo Y. Longitudinal vibration analysis of wheelset on locomotive under slippage. *J Mech Engng* 2009; 45: 199–203.
8. Yao Y, Zhang HJ and Chen K. Self-excited torsional vibrations of drive system on locomotive under slippage. *J Southwest Jiaotong Univ* 2008; 43: 762–766.

9. Zhang WH, Chen JZ and Wu XJ. Wheel/rail adhesion and analysis by using full scale roller rig. *Wear* 2002; 253: 82–88.
10. Koansok B, Keiji K and Tsunamitsu N. An experimental investigation of transient traction characteristics in rolling–sliding wheel/rail contacts under dry–wet conditions. *Wear* 2007; 263: 169–179.
11. Polach O. A fast wheel-rail force calculation computer code. *Veh Syst Dyn* 1999; 33: 728–739.
12. Ertz M and Knothe K. Thermal stresses and shakedown in wheel/rail contact. *Arch Appl Mech* 2003; 72: 1521–1533.
13. Lata M. The modern wheelset drive system and possibilities of modelling the torsion dynamics. *Transport* 2008; 23: 172–181.
14. Jin XS and Zhang LM. Numerical analysis of the driving torque applied to a single wheelset of locomotive with high speed. *Chin J Mech Engng* 1999; 35: 56–60.
15. Shen ZY, Hedrick JK and Elkins JA. A comparison of alternative creep-force models for rail vehicle dynamic analysis. *Veh Sys Dyn* 1983; 12: 79–83.
16. Mei TX, Yu JH and Wilson DA. Wheelset dynamics and wheel slip detection. In: *The international symposium on speed-up and service technology for railway and maglev systems*, (ed S Zhiyun), Chengdu, China, 11–15 August 2006. China: Southwest Jiaotong University Press, pp.221–225.
17. Leva S, Morando AP and Colombaioni P. Dynamic analysis of a high-speed train. *Veh Technol* 2008; 57: 107–119.
18. Sun K, Uk H and Hak K. Re-adhesion control with estimated adhesion force coefficient for wheeled robot using fuzzy logic. In: *The 30th annual conference of the IEEE Industrial Electronics Society*, Busan, South Korea, 2–6 November 2004. Piscataway, NJ: IEEE Press, pp.2530–2535.